



HAL
open science

Metabotropic glutamate receptor subtype 1 regulates sodium currents in rat neocortical pyramidal neurons

Edmond Carlier, Valérie Sourdet, Sami Boudkkazi, Patrice Déglise, Norbert Ankri, Laure Fronzaroli-Molinieres, Dominique Debanne

► To cite this version:

Edmond Carlier, Valérie Sourdet, Sami Boudkkazi, Patrice Déglise, Norbert Ankri, et al.. Metabotropic glutamate receptor subtype 1 regulates sodium currents in rat neocortical pyramidal neurons. *The Journal of Physiology*, 2006, 577 (1), pp.141-154. 10.1113/jphysiol.2006.118026 . hal-01766852

HAL Id: hal-01766852

<https://amu.hal.science/hal-01766852>

Submitted on 25 Apr 2018

HAL is a multi-disciplinary open access archive for the deposit and dissemination of scientific research documents, whether they are published or not. The documents may come from teaching and research institutions in France or abroad, or from public or private research centers.

L'archive ouverte pluridisciplinaire **HAL**, est destinée au dépôt et à la diffusion de documents scientifiques de niveau recherche, publiés ou non, émanant des établissements d'enseignement et de recherche français ou étrangers, des laboratoires publics ou privés.

Metabotropic glutamate receptor subtype 1 regulates sodium currents in rat neocortical pyramidal neurons

Edmond Carlier^{1,2}, Valérie Sourdet^{1,2}, Sami Boudkkazi^{1,2}, Patrice Déglise^{1,2}, Norbert Ankri^{1,2}, Laure Fronzaroli-Molinieres^{1,2} and Dominique Debanne^{1,2}

¹INSERM U641, Marseille, F-13916 France

²Université de la Méditerranée, Faculté de médecine secteur nord, IFR 11, Marseille, F-13916 France

Brain sodium channels (NaChs) are regulated by various neurotransmitters such as acetylcholine, serotonin and dopamine. However, it is not known whether NaCh activity is regulated by glutamate, the principal brain neurotransmitter. We show here that activation of metabotropic glutamate receptor (mGluR) subtype I regulates fast transient (I_{NaT}) and persistent Na^+ currents (I_{NaP}) in cortical pyramidal neurons. A selective agonist of group I mGluR, (S)-3,5-dihydroxyphenylglycine (DHPG), reduced action potential amplitude and decreased I_{NaT} . This reduction was blocked when DHPG was applied in the presence of selective mGluR1 antagonists. The DHPG-induced reduction of the current was accompanied by a shift of both the inactivation curve of I_{NaT} and the activation curve of I_{NaP} . These effects were dependent on the activation of PKC. The respective role of these two regulatory processes on neuronal excitability was determined by simulating transient and persistent Na^+ conductances (G_{NaT} and G_{NaP}) with fast dynamic-clamp techniques. The facilitated activation of G_{NaP} increased excitability near the threshold, but, when combined with the down-regulation of G_{NaT} , repetitive firing was strongly decreased. Consistent with this finding, the mGluR1 antagonist LY367385 increased neuronal excitability when glutamatergic synaptic activity was stimulated with high external K^+ . We conclude that mGluR1-dependent regulation of Na^+ current depresses neuronal excitability, which thus might constitute a novel mechanism of homeostatic regulation acting during intense glutamatergic synaptic activity.

Corresponding author D. Debanne: Université de la Méditerranée, Faculté de médecine secteur nord, IFR 11, Marseille, F-13916 France. Email: debanne.d@jean-roche.univ-mrs.fr

In central neurons, sodium channels (NaChs) set the threshold for action potential (AP) generation and are therefore crucial in the control of neuronal excitability. Although early studies indicated that NaChs were not subject to modulation (reviewed in Cantrell & Catterall, 2001), there is now growing evidence showing that NaChs are regulated upon activation of several receptors such as muscarinic acetylcholine (Cantrell *et al.* 1996), dopamine (Cantrell *et al.* 1999; Cantrell & Catterall, 2001), serotonin (Carr *et al.* 2002, 2003) and tyrosine kinase-associated receptors (Hilborn *et al.* 1998; Ratcliff *et al.* 2000). Most of these regulations are mediated by phosphorylation of the intracellular loops of the α -subunit of the NaCh. NaChs are down-regulated in central neurons by phosphorylation on serine/threonine residues by cAMP-dependent protein kinase (PKA) and protein kinase C (PKC) (Sigel & Baur, 1988; Numann *et al.* 1991; Li *et al.* 1992; Cantrell *et al.* 1997; Franceschetti *et al.* 2000). Furthermore, the sodium current mediated by $\text{Na}_v1.6$, the major sodium channel isoform at nodes

of Ranvier in myelinated axons, is down-regulated by p38 mitogen-activated protein kinase (Wittmack *et al.* 2005). Finally, Ca^{2+} /calmoduline-dependent kinase II regulates NaCh activity (Carlier *et al.* 2000).

Although several neurotransmitters modulate NaCh activity through G-protein signalling cascades or direct G-protein interaction, the effects of glutamate have surprisingly not yet been considered in central neurons. Group I metabotropic glutamatergic receptors (mGluRs) (mGluR1 and mGluR5) stimulate phosphatidylinositol diphosphate hydrolysis and intracellular Ca^{2+} release that leads to the activation of PKC (Conn & Pin, 1997). Thus, activation of group I mGluRs may also regulate NaCh activity. Activation of group I mGluRs increases cortical excitability (Charpak *et al.* 1990) and prolongs epileptiform bursts (Merlin & Wong, 1997; Merlin, 2002). Classically, this enhanced neuronal excitability is thought to be mediated by the regulation of a wide range of K^+ , Ca^{2+} and cationic currents (Anwyl, 1999). However, it is still unknown whether the mGluR-dependent increment

in excitability could be mediated by regulation of NaCh activity.

We investigated here the consequence of specific mGluR stimulation on NaCh activity in acutely dissociated neocortical pyramidal neurons and in L5 pyramidal neurons recorded in neocortical slices. We show that activation of mGluR1 regulates I_{NaT} and I_{NaP} in neocortical pyramidal neurons via a PKC-dependent mechanism. In the presence of an mGluR1 agonist, steady-state inactivation of I_{NaT} increased producing a reduction of I_{NaT} whereas I_{NaP} was facilitated via a leftward shift in its activation. In order to determine the net effect of these processes on neuronal excitability we used the fast dynamic-clamp (FDC) technique to reproduce independently modulation of G_{NaT} or G_{NaP} . We show here that the net effect is a reduction of the first spike latency associated with the suppression of repetitive firing. Functionally, the mGluR1-dependent regulation of Na^+ current might constitute a novel mechanism of homeostatic regulation acting during regimes of high synaptic activity.

Methods

Acute dissociation of cortical neurons

Most voltage-clamp recordings were obtained from isolated cortical neurons. Cortical slices (350 μm) were obtained from postnatal day 11–18 Wistar rats, as described elsewhere (Sourdet *et al.* 2003). All experiments were carried out according to the European and institutional guidelines for the care and use of laboratory animals (Council Directive 86/609/EEC and French National Research Council). Rats were deeply anaesthetized with chloral hydrate (intraperitoneal, 200 mg kg^{-1}) and killed by decapitation. Slices were cut in an ice-cold solution containing (mM): 280 sucrose, 26 NaHCO_3 , 10 D-glucose, 10 MgCl_2 , 1.3 KCl, 1 CaCl_2 , and were bubbled with 95% O_2 –5% CO_2 , pH 7.4. Slices recovered (1 h) in a solution containing (mM): 125 NaCl, 26 NaHCO_3 , 3 CaCl_2 , 2.5 KCl, 2 MgCl_2 , 0.8 NaH_2PO_4 , 10 D-glucose, oxygenated and the pH adjusted to 7.4 with 95% O_2 –5% CO_2 . The slices were transferred to a treatment chamber containing pronase E (Sigma protease type XIV, 1.0 mg ml^{-1}) and (mM): 114 NaCl, 1 CaCl_2 , 1 NaH_2PO_4 , 8 MgCl_2 , 2.5 KCl, 20 glucose, 10 Hepes, 2 kynurenic acid, pH 7.3–7.4. Neurons were mechanically dissociated in a solution containing (mM): 140 Na-isothionate, 2 KCl, 4 MgCl_2 , 0.1 CaCl_2 , 23 glucose, 15 Hepes, 1 kynurenic acid, pH 7.3–7.4. The cell suspension was placed in recording solution and transferred to the stage of the microscope. Pyramidal-like neurons with short neurites were selected for this study. Electrophysiological recordings were performed at 22–27°C. Recordings of fast-inactivating sodium current (I_{NaT}) were performed

with a reduced external Na^+ concentration to minimize the impact of eventual series-resistance induced errors (Huguenard *et al.* 1988). The external solution contained (mM): 10 NaCl, 110 mM choline chloride, 20 tetraethylammonium (TEA)-Cl, 2 MgCl_2 , 1.3 CaCl_2 , 3 KCl, 0.4 CdCl_2 , 0.3 NiCl_2 , 2 kynurenic acid, 10 glucose and 10 Hepes (pH 7.3–7.4). Pipettes were filled with an intracellular solution containing (mM): 75 CsF, 55 CsCl, 1 MgCl_2 , 10 EGTA, 10 Hepes, 3 Na_2ATP , 10 phosphocreatine and 20 unit ml^{-1} creatinine phosphokinase, pH 7.3. In the whole-cell configuration, the access resistance was $4.6 \pm 0.2 \text{ M}\Omega$ ($n = 33$). Whole-cell currents were recorded with an Axopatch 200A (Axon Instruments), low-pass filtered at 4 kHz and sampled at 20 kHz. Capacitance transients were cancelled and series resistances were compensated (> 80%). Remaining capacitance and leak currents were subtracted with an on-line P/4 protocol. The voltage control was considered to be adequate when the latency of the peak Na^+ current did not vary more than 1 ms at the activation threshold and when the activation was a continuous function of voltage (Huguenard *et al.* 1988). In all other cases, the recordings were not considered for the final analysis. Persistent sodium currents were recorded with a normal external Na^+ concentration (120 mM Na^+ ; 0 mM choline chloride). Data acquisition and analysis were controlled by pCLAMP8 software (Axon Instruments).

Recordings from L5 pyramidal neurons

All current-clamp and dynamic-clamp recordings were obtained from L5 pyramidal neurons in slices. Cortical slices (350 μm) were prepared as described above. Each slice was transferred to a submerged chamber mounted on an upright microscope. L5 pyramidal neurons were visualized using DIC infrared videomicroscopy. Whole-cell recordings were made at room temperature (22–25°C). Patch pipettes (8–10 $\text{M}\Omega$) were filled with the following solution (mM): 120 K-gluconate, 20 KCl, 10 Hepes, 0.5 EGTA, 2 Na_2ATP and 2 MgCl_2 , pH 7.4. Recordings were made with appropriate bridge and capacitance compensation (series resistances: 15–30 $\text{M}\Omega$). The external solution contained (mM): 125 NaCl, 26 NaHCO_3 , 3 CaCl_2 , 2 MgCl_2 , 2.5 KCl, 0.8 NaH_2PO_4 , 10 D-glucose and was equilibrated with 95% O_2 –5% CO_2 . Kynurenic acid (2 mM) and picrotoxin (100 μM) were applied to block excitatory and inhibitory synaptic events. Pharmacologically isolated Na^+ action potentials were recorded in the presence of 200 μM NiCl_2 , 200 μM CdCl_2 , 2 mM 4-AP and 20 mM TEA.

Analog signals were low-pass filtered at 3 kHz and acquisition of 800 ms sequences was performed at 12 kHz. In current-clamp recordings, trials with membrane potential fluctuation greater than 1 mV were discarded. Pooled data are expressed as means \pm s.e.m. and statistical

significance was accepted at the $P < 0.05$ level in various tests.

Drugs

1S,3R-Aminocyclopentane-1,3-dicarboxylate (1S,3R-ACPD), (R,S)-2-chloro-5-hydroxyphenyl glycine (CHPG) (S)-3,5-dihydroxyphenylglycine (DHPG), 2-methyl-6-phenylethynyl-pyridine (MPEP), (+)-2-methyl-4-carboxy-phenyl-glycine (LY367385), 7-(hydroxyimino)cyclopropal(b)chromen-1a-carboxylate ethyl ester (CPCCOEt), and R(-)-1-amino-2,3-dihydro-1H-indene-1,5-dicarboxylic acid (AIDA) were purchased from Tocris Cookson, Inc. Bisindolylmaleimide I (Bis-I), picrotoxin, kynurenate, TEA, 4-AP, NiCl₂ and CdCl₂ were obtained from Sigma. Tetrodotoxin (TTX) was purchased from Latoxan. The protein kinase C inhibitor peptide 19–36 was obtained from Calbiochem.

Description of Na⁺ channel gating with an HH-type model

Equations describing the voltage dependence of G_{NaT} were based on a deterministic Hodgkin-Huxley model with three variables which obey first order kinetics. m , h and s are the gating particle for activation, and fast and slow inactivation, respectively. The transient Na⁺ current is given by:

$$I_{\text{NaT}} = G_{\text{NaT}}(V_m - E_{\text{Na}})$$

where V_m is the membrane potential, E_{Na} is the equilibrium potential for Na⁺ ($E_{\text{Na}} = +15$ mV in Figs 4 and 5 and $E_{\text{Na}} = +50$ mV in dynamic-clamp experiments, Fig. 6), and G_{NaT} is the transient Na⁺ conductance:

$$G_{\text{NaT}} = G_{\text{NaTmax}} m^3 h s$$

The activation and fast inactivation time constants were determined by fitting experimental Na⁺ currents recorded in three cells with the function:

$$I = A(1 - \exp(-t/\tau_m))^3 \exp(-t/\tau_h)$$

where $A = G_{\text{NaTmax}} m_\infty^3 h(0)$, and τ_m and τ_h are the activation and inactivation time constants, respectively (see online Supplemental material Fig. 1 for details). Activation and inactivation curves were fitted with the Boltzmann function:

$$1/(1 + \exp((V - V_{1/2})/k)).$$

where $V_{1/2}$ is the potential at which the value of the function is 0.5 and k is the slope of the Boltzmann function. For activation, $V_{1/2} = -37$ mV and $k = -5.2$, and for inactivation, $V_{1/2} = -55$ mV and $k = 6.9$.

For $x = \{m, h, s\}$

$$dx/dt = \alpha_x(1 - x) - \beta_x x$$

$$x_\infty = \alpha_x/(\alpha_x + \beta_x)$$

$$\tau_x = 1/(\alpha_x + \beta_x)$$

$$\alpha_m = 0.55(V + 37)/(1 - \exp(-(V + 37)/5.2))$$

$$\beta_m = 0.55(V + 37)/(\exp(((V + 37)/5.2) - 1))$$

$$\alpha_h = 0.015(V + 55)/(\exp((V + 55)/6.9) - 1)$$

$$\beta_h = 0.015(V + 55)/(1 - \exp(-(V + 55)/6.9))$$

The coefficients 0.55 and 0.015 were adjusted to fit the experimental decay.

The variable s accounted for the slow inactivation of the Na⁺ current observed experimentally. s was described by the following equations (adapted from Fleidervish *et al.* 1996):

$$\alpha_s = 0.01 \exp((-85 - V)/30)$$

$$\beta_s = 0.034/(\exp((-17 - V)/10) + 1)$$

G_{NaP} was modelled by the equation: $G_{\text{NaP}} = G_{\text{NaPmax}} m_P^3$

The gating particle, m_P was directly described by the equation:

$$m_P(V) = 1/(1 + \exp[-(V - V_{P,1/2})/k_P])$$

with $V_{P,1/2} = -48$ mV and $k_P = 3.3$ determined experimentally.

In order to avoid bursting behaviour caused by the reduction of Na⁺-dependent K⁺ currents due to TTX (Bhattachardjee & Kaczmarek, 2005), a delayed rectifier voltage-gated potassium conductance was added. This delayed rectifier was introduced by the following equations (Fleidervish *et al.* 1996):

$$I_K = G_K n^4 (V_m - E_K)$$

where the equilibrium potential for K⁺ (E_K) = -90 mV.

$$dk/dt = \alpha_k(1 - k) - \beta_k k$$

$$k_\infty = \alpha_k/(\alpha_k + \beta_k)$$

$$\tau_k = 1/(\alpha_k + \beta_k)$$

$$\alpha_k = 0.034(V + 45)/(1 - \exp(-(V + 45)/5))$$

$$\beta_k = 0.54 \exp((-75 - V)/40)$$

Dynamic clamp

To add artificial I_{Na} conductance to real L5 neurons, a fast dynamic-clamp (FDC) system was developed (Kullmann *et al.* 2004; Prinz *et al.* 2004). The system consisted of an embedded processor (National Instruments 8176, 1.26 GHz Pentium II processor, 128 MB RAM, 15 GB Fast ATA 100 hard disk) with real time operating system which was programmed and controlled from a host PC with the graphical programming language LabView-7-Express containing the LabView Real-Time module. The feedback loop ($F = 38$ kHz) continuously read the membrane potential V from the Axoclamp 2B, computed G_{NaT} and generated an output, I_{NaT} according to the equation: $I_{\text{NaT}} = G_{\text{NaT}}(V - E_{\text{Na}})$. A reconfigurable I/O

module (NI PXI-7831R) allowed monitoring of V and generation of I_{NaT} . The access speed of analog–digital and digital–analog conversions on the input/output module was optimized by a field-programmable gate array (FPGA).

To minimize calculations during the calculation loop, specific arrays of $\tau_x(V)$, $x_\infty(V)$ and $A_x(V) = 1 - \exp(\Delta t/\tau_x)$ were initialized with a resolution of 0.1 mV. For a given voltage, corresponding values of $\tau_x(V)$, $x_\infty(V)$ and $A_x(V)$ were obtained by linear interpolation from the array. The numerical integration based on Euler's method involved a simple linear extrapolation of the gating variable given by the equation:

$$x_{k+1} = x_k + (x_\infty - x_k)A_x$$

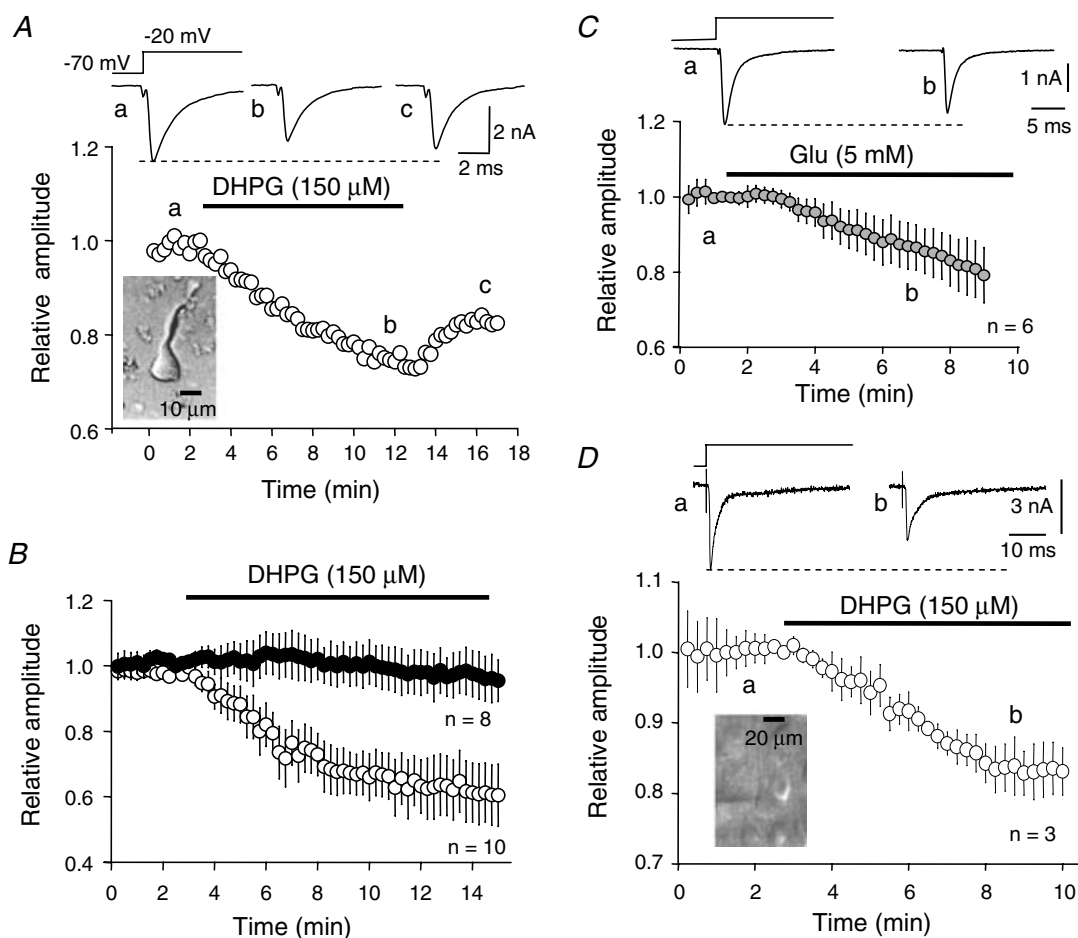


Figure 1. DHPG or glutamate inhibits fast inactivating Na⁺ current in neocortical pyramidal neurons

Aa, the normalized value of peak inward Na⁺ current evoked by a voltage step from -70 to -20 mV in an acutely dissociated neocortical neuron (see inset) is plotted as a function of time. *b*, bath application of DHPG (150 μM) induced a 25% reduction of the amplitude that partially recovered after washout (*c*). *B*, plot of average (mean ± s.e.m.) normalized peak current evoked by a step from a holding potential of -70 mV to -20 mV as a function of time. DHPG induced a stable depression of the Na⁺ current (○). Peak amplitude was stable in control experiments (●). *C*, inhibition of the Na⁺ current induced by glutamate. Top, representative Na⁺ currents evoked by a step from -70 to -20 mV. Bottom, time course of the inhibition. *D*, in L5 pyramidal neurons (inset), DHPG induced a 20% reduction in the peak Na⁺ current amplitude evoked by a voltage step from -70 to -20 mV. External Na⁺ concentration: 125 mM.

Similar operations were performed to inject G_{NaP} and G_{K} for which specific arrays of $m_{\text{P}}(V)$ and $n(V)$ were generated with a resolution of 0.1 mV.

An Axoclamp 2B amplifier (Axon Instruments) was used for dynamic-clamp experiments. To avoid series resistance artifacts, dual current-clamp whole-cell recordings were made, allowing us to separate the current-feeding from the whole-cell recording electrode (Lien & Jonas, 2003). Only recordings with series resistance $< 25 \text{ M}\Omega$ (mean $13 \pm 4 \text{ M}\Omega$) were kept for further analysis.

Endogenous Na^+ currents were blocked with 0.1–0.2 μM TTX and the transient and persistent components of the Na^+ conductance were simulated with the FDC. The maximal conductances G_{NaTmax} , G_{NaPmax} and G_{Kmax} were adjusted to reproduce the firing behaviour of the neuron. The values of G_{NaTmax} , G_{NaPmax} and G_{Kmax} were on average $3100 \pm 177 \text{ nS}$, $3.7 \pm 0.3 \text{ nS}$ and $120 \pm 16 \text{ nS}$ ($n = 5$). An external digital device (microcontroller PIC-16F876A (Microchip®)) was used to facilitate the adjustment of the values of G_{NaTmax} , G_{NaPmax} , G_{Kmax} , τ_{h} (inactivation of G_{NaT}) and τ_{mP} (activation of G_{NaP}) during the experiment. Thus, digitized values of these variables were directly read in real time by the I/O module.

Results

Down-regulation of the transient sodium current (I_{NaT}) by mGluR1

Whole-cell patch-clamp recordings were obtained from acutely dissociated pyramidal neurons (ADPNs) to study the fast inactivating sodium current (I_{NaT}). In this case, voltage-clamp recordings were obtained with a reduced external Na^+ concentration. Bath application of the mGluR1/5 agonist DHPG produced a partially reversible reduction in the peak amplitude of I_{NaT} evoked by a step from a holding potential of -70 mV to a command potential of -20 mV (Fig. 1A). This reduction was dose dependent, yielding an EC_{50} of $54 \mu\text{M}$ (see Supplemental material Fig. 2). At saturating concentrations ($150 \mu\text{M}$), the mean inhibition was $-38 \pm 9\%$ ($n = 10$, paired t test, $P < 0.001$, Fig. 1B). In control cells, I_{NaT} was stable for the duration of the recording ($97 \pm 1\%$ of the control amplitude at +10 min, $n = 8$, paired t test $P > 0.2$, Fig. 1B). Glutamate similarly reduced the amplitude of I_{NaT} recorded in ADPNs ($-13 \pm 6\%$, $2989 \pm 789 \text{ pA}$ vs. $2598 \pm 718 \text{ pA}$ in the presence of 5 mM glutamate, $n = 6$, $P < 0.02$; Fig. 1C). Reduction of I_{NaT} was also induced by mGluR activation in L5 pyramidal neurons recorded in acute slices of the sensori-motor cortex. Bath application of DHPG ($150 \mu\text{M}$) induced a reduction of I_{NaT} ($-18 \pm 5\%$, $n = 3$ paired t test $P < 0.01$, Fig. 1D).

The regulation of the transient sodium current had visible effects on the action potential waveform recorded from pyramidal neurons *in situ*. DHPG ($150 \mu\text{M}$)

decreased the rate of depolarization of the spike (maximal dV/dt : $173 \pm 40 \text{ mV ms}^{-1}$ in control vs. $122 \pm 27 \text{ mV ms}^{-1}$ in DHPG, $n = 6$, paired t test $P < 0.01$) and reduced its amplitude ($83 \pm 3 \text{ mV}$ in control vs. $76 \pm 4 \text{ mV}$ in DHPG, $n = 6$, paired t test, $P < 0.01$; Fig. 2).

DHPG is an agonist of both mGluR1 and mGluR5. Thus, we characterized in ADPN the mGluR subtype involved in this regulation. No inhibition of I_{NaT} was observed when DHPG ($75 \mu\text{M}$) was applied in the presence of the mGluR1 antagonists LY367385 ($150 \mu\text{M}$, $-2 \pm 4\%$, $n = 9$, paired t test $P > 0.2$), CPCCOEt ($50 \mu\text{M}$, $13 \pm 4\%$, $n = 6$, paired t test $P < 0.001$) and AIDA ($100 \mu\text{M}$, $11 \pm 8\%$, $n = 5$, paired t test $P > 0.2$, Fig. 3A). We next determined the contribution of mGluR5. In contrast to the preceding results, DHPG ($75 \mu\text{M}$) applied in the presence of the selective mGluR5 antagonist MPEP ($10 \mu\text{M}$) induced a significant inhibition of I_{NaT} ($-23 \pm 5\%$, $n = 5$, paired- t test $P < 0.02$). To further confirm that the reduction of I_{NaT} was not due to the activation of mGluR5, we tested the effect of the selective mGluR5 agonist CHPG. Even high concentrations of CHPG ($500 \mu\text{M}$) did not induce any reduction of the peak current ($6 \pm 7\%$ $n = 8$, paired t test $P > 0.2$, Fig. 3B). The lack

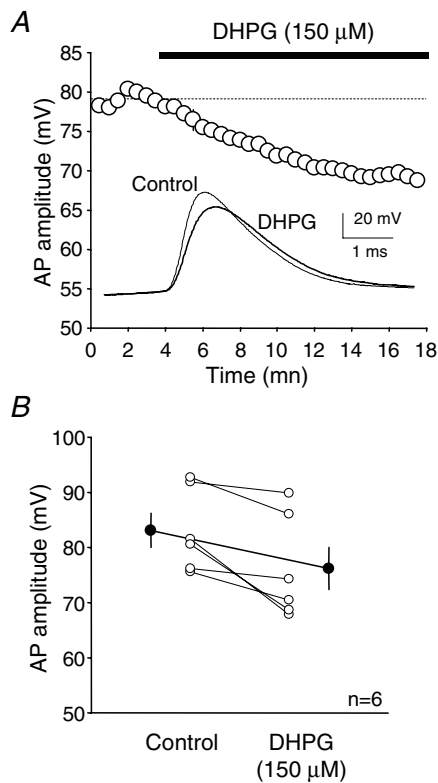


Figure 2. DHPG reduces the amplitude of the action potential in L5 pyramidal neurons

A, effect of $150 \mu\text{M}$ DHPG on action potential amplitude. B, summary of the changes in AP amplitude in control and in the presence of DHPG (measured after 10 min).

of effect was not due to the inefficiency of the mGluR5 agonist. CHPG had a significant impact on the intrinsic excitability of L5 pyramidal neurons and increased the spike number elicited by current pulses ($127 \pm 13\%$, $n = 3$ with $100 \mu\text{M}$ CHPG and $143 \pm 8\%$ with $200 \mu\text{M}$ CHPG, $n = 3$, Supplemental material Fig. 3). We thus conclude that the down-regulation of I_{NaT} is mediated by mGluR1.

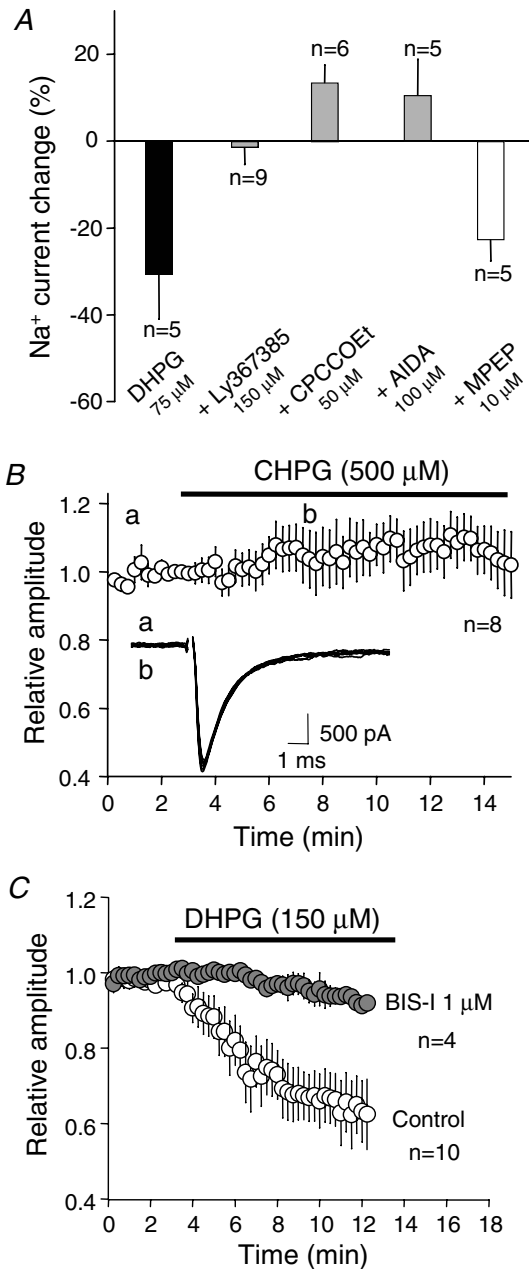


Figure 3. Pharmacological profile of the DHPG-induced reduction in peak current

A, the DHPG-induced inhibition was blocked by mGluR1 antagonists (Ly367385, CPCCOEt and AIDA) but not by the mGluR5 antagonist MPEP. B, effect of the mGluR5 agonist CHPG on I_{NaT} evoked by a step from -70 to -20 mV. C, effect of DHPG on I_{NaT} in the presence of the PKC inhibitor BIS-I.

It is well established that mGluR1 stimulation leads to activation of protein kinase C (Conn & Pin, 1997). NaChs contain consensus sequences for PKC phosphorylation that lead to a decrease in I_{NaT} (Cantrell & Catterall, 2001). The application of DHPG ($150 \mu\text{M}$) in the presence of the broad spectrum PKC antagonist BIS-I ($1 \mu\text{M}$) had virtually no effect on I_{NaT} recorded in ADPNs ($-7 \pm 2\%$, $n = 4$, paired t test $P > 0.05$; Fig. 3C). Furthermore, when neurons were recorded with the PKC inhibitory peptide 19–36 in the patch pipette ($4 \mu\text{M}$) DHPG had no effect on transient currents evoked by a step from -70 mV to -20 mV (1039 ± 188 pA in control vs. 1086 ± 235 pA, $n = 4$, paired t test $P > 0.2$). Thus, the down-regulation of I_{NaT} current induced by mGluR1 is mediated by the activation of PKC.

Activation of mGluR1 induces a negative shift in I_{NaT} inactivation

In order to identify the biophysical process underlying the reduction of I_{NaT} , we next characterized the effects of DHPG on steady-state activation and inactivation. In the presence of DHPG ($150 \mu\text{M}$), the peak current amplitude recorded in ADPN was reduced (Fig. 4A) but the activation curves in control and in the presence of DHPG were virtually identical (Fig. 4B), indicating that stimulation of mGluR1 does not change steady-state activation.

Inactivation was tested by stepping from potentials between -120 mV and -10 mV (prepulse duration of 100 ms) to -20 mV. A negative shift in inactivation was observed in the presence of DHPG (Fig. 4C). In fact, DHPG reduced the peak current evoked by a voltage step to -20 mV when the holding potential (V_{H}) was -50 mV (1254 ± 380 pA vs. 692 ± 218 pA in the presence of DHPG, $n = 6$ cells) but no significant reduction was observed when inactivation was removed by setting V_{H} to -120 mV (2382 ± 648 pA vs. 2350 ± 705 pA in the presence of DHPG, $n = 6$ cells). Half-inactivation was obtained for a mean potential of -53.8 mV in control conditions and -63.3 mV in the presence of DHPG (the DHPG-induced shift of $V_{1/2}$ ranged between -4 and -12 mV, $n = 6$). To further confirm that this shift could underlie the decrease in peak amplitude, G_{NaT} was modelled (see Methods). The model showed that a leftward shift in the inactivation from -55 to -64.5 mV was associated with a 25% reduction of I_{NaT} amplitude (Fig. 4D). We conclude that the DHPG-induced decrease in the amplitude of I_{NaT} is mainly mediated by a negative shift of the inactivation curve.

DHPG regulates I_{NaP}

In neocortical pyramidal neurons, persistent Na^+ current (I_{NaP}) controls excitability and excitatory postsynaptic potential (EPSP) amplification (Schwindt & Crill, 1995;

Stuart & Sakmann, 1995). The narrow window of potential between activation and inactivation curves of I_{NaT} generates a persistent current usually called the 'window current' (I_{NaPW}). This current represents nearly a third of the total I_{NaP} (Magistretti & Alonso, 1999; Maurice *et al.* 2001). Since DHPG shifts the inactivation

curve of I_{NaT} towards negative values without changing the activation, I_{NaPW} amplitude might be affected. Indeed, the model shows that G_{NaPW} calculated as the product of the activation and steady-state inactivation functions was dramatically reduced when inactivation was shifted by 9.5 mV (Fig. 5A).

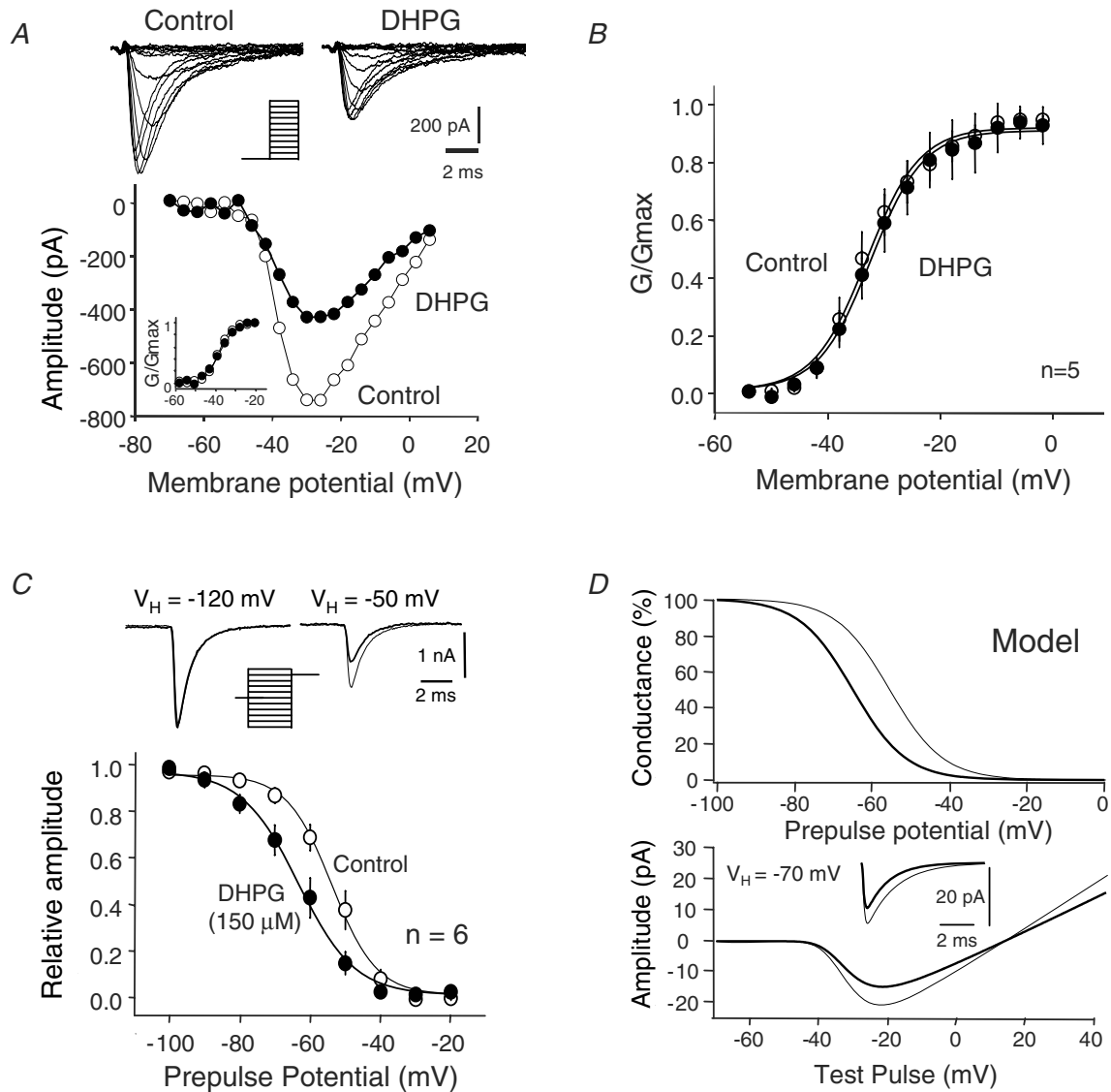


Figure 4. Effect of DHPG on activation and steady-state inactivation of I_{NaT}

A, DHPG does not affect activation of I_{NaT} . Upper traces, families of Na^+ currents recorded with a reduced Na^+ gradient in control and in the presence of DHPG (150 μM). Lower graph, current-voltage plots in control (o) and in the presence of DHPG (\bullet). Inset, normalized activation curves in control ($V_{1/2} = -37.4$ mV; slope factor: 3.1 mV/e-fold) and the presence of DHPG ($V_{1/2} = -36.8$ mV and $k = 3.9$ mV/e-fold). B, pooled data over 5 cells. Plot of I_{NaT} activation curves under control conditions (o, $V_{1/2} = -33$ mV, slope factor: 4.7 mV/e-fold) and in the presence of DHPG (\bullet , $V_{1/2} = -31$ mV, slope factor: 4.6 mV/e-fold). C, effect of DHPG on steady-state inactivation of I_{NaT} recorded with a reduced gradient. DHPG shifted the voltage dependence of steady-state inactivation to more negative values. Half-inactivation was obtained for a holding potential of -53.8 mV in control (o, slope factor: -6.4 mV/e-fold) vs. -63.3 mV in the presence of DHPG (\bullet , slope factor: -8.0 mV/e-fold). D, model of the transient Na^+ conductance ($G_{NaTmax} = 1$ nS, in this case, $E_{Na} = +15$ mV). Upper graph, theoretical inactivation curves; lower graph, $I-V$ curves. A 25% reduction of the peak current amplitude is produced when the steady-state inactivation is shifted by -9.5 mV.

We next determined whether DHPG also reduced I_{NaP} in ADPNs. I_{NaP} was evoked by a depolarizing ramp (Fig. 5B). This current was totally blocked by TTX, indicating that it was mediated by NaChs. The maximal amplitude of G_{NaP} amounted to 0.62 ± 0.04 nS ($n = 36$). The addition of $150 \mu\text{M}$ DHPG induced a consistent leftward shift of the voltage dependence of I_{NaP} . Half-maximal activation

was obtained for a potential of -48.2 mV in control and -54.7 mV in the presence of DHPG ($n = 7$). An increase in the current amplitude was observed between -60 and -50 mV. This current was totally blocked by TTX and thus did not correspond to the TTX-resistant inward voltage-gated current described by Chuang *et al.* (2000). In contrast to model predictions on G_{NaPW} , the peak

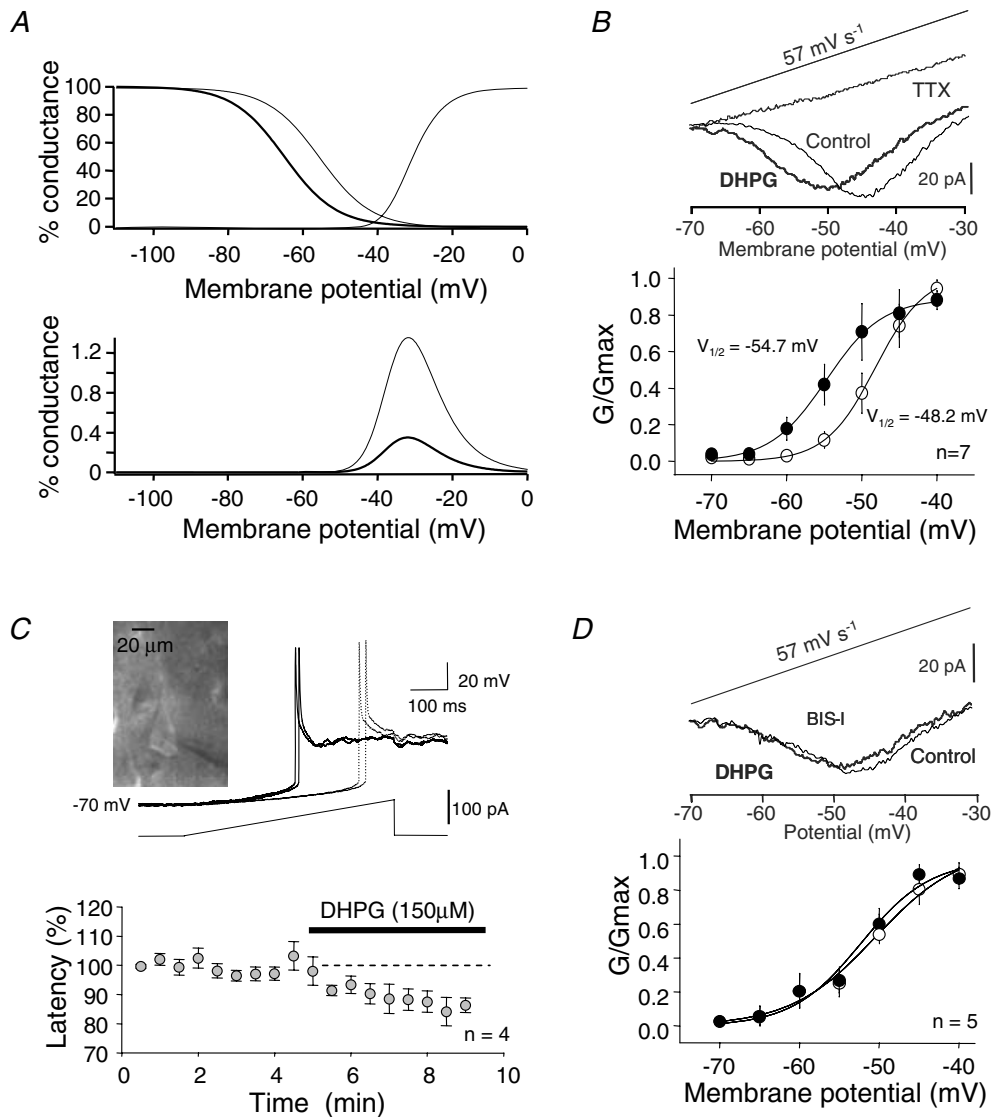


Figure 5. DHPG-induced regulation of I_{NaP}

A, theoretical impact of the shift of the steady-state inactivation on the persistent sodium conductance (same model as in Fig. 4D). Upper graph, activation and inactivation curves. Lower graph, resulting window Na^+ conductance in control (thin line) and after the -9.5 mV shift in the inactivation curve (thick line). B, regulation of I_{NaP} in acutely dissociated neurons evoked by a ramp of voltage (leak and capacitive currents were not subtracted). Upper panel, DHPG shifted the activation of I_{NaP} evoked by a slow ramp of voltage to more negative values. The current was totally blocked by TTX ($1 \mu\text{M}$). Bottom, I_{NaP} activation curve. Half-maximal activation of I_{NaP} was obtained for -48.2 mV in control (○) vs. -54.7 mV in the presence of DHPG (●). C, current-clamp recording in L5 pyramidal neurons. Single APs were evoked by a slow ramp of current in the presence of K^+ and Ca^{2+} channel blockers. Application of DHPG decreased the AP latency. Bottom, plot of average (mean \pm s.e.m.) normalized latency as a function of time. D, effect of DHPG on I_{NaP} in the presence of BIS-I ($1 \mu\text{M}$). Leak and capacitive currents were not subtracted. No shift in the activation of I_{NaP} was induced by DHPG (lower graph). (○) control (●) DHPG.

amplitude of I_{NaP} was not significantly reduced but the current was depressed at -40 mV, suggesting that DHPG depressed the window current but facilitated activation of the non-window current. In the presence of the mGluR1 agonist LY367385 ($150 \mu\text{M}$), DHPG ($75 \mu\text{M}$) produced no effect on the activation of I_{NaP} (-47.3 ± 0.8 mV *vs.* $V_{1/2} = -45.0 \pm 1.2$ mV $n = 4$ in control; $P > 0.1$, data not shown). Furthermore, CHPG ($500 \mu\text{M}$) had no effect on the activation of I_{NaP} ($V_{1/2} = -51.5 \pm 1.1$ mV in control and -51.4 ± 0.9 mV in the presence of CHPG, $n = 4$, $P > 0.1$), indicating that the observed regulation of I_{NaP} was mediated by mGluR1.

If activation of I_{NaP} is facilitated by DHPG, then excitability should be enhanced. Pharmacologically isolated Na^+ APs were elicited by slow depolarizing ramps of current in L5 pyramidal neurons recorded in neocortical slices. DHPG ($150 \mu\text{M}$) produced an increase in the amplitude of the spike prepotential preceding the AP and subsequently reduced its latency ($84 \pm 5\%$ of the control latency, $n = 4$, Fig. 5C). These data confirm that DHPG facilitates activation of I_{NaP} and enhances intrinsic excitability.

We next tested whether regulation of I_{NaP} was also mediated by activation of PKC in ADPN. Neither change in I_{NaP} amplitude nor change in its activation curve was observed in the presence of the PKC-inhibitor, BIS-I (Fig. 5D). We conclude that both the reduction of I_{NaT} and the leftward shift in the activation of I_{NaP} are mediated by a signalling cascade involving the activation of PKC.

Net functional effect on intrinsic excitability

The mGluR1-induced reduction of I_{NaT} might decrease intrinsic excitability whereas the facilitation of I_{NaP} should have opposite effects. The resulting change in excitability is rather difficult to determine experimentally since mGluR1 also regulates a wide variety of K^+ channels that may in turn also regulate neuronal excitability. We took advantage of the FDC technique to reproduce the regulation of I_{NaT} and I_{NaP} independently while other voltage-gated currents remained virtually unchanged. Double whole-cell recordings were obtained from the soma of L5 pyramidal neurons in slices. Endogenous NaChs were blocked with TTX (100 – 200 nM) and G_{NaT} and G_{NaP} were simulated with the FDC. G_{K} was added to reduce bursting behaviour caused by the reduction of Na^+ -dependent K^+ currents due to TTX (Fig. 6A and B).

In our model, I_{NaPW} produced a persistent component that contributed 1.3% of the maximal transient component (Fig. 4A). However, G_{NaPW} represents only a fraction of G_{NaP} evoked by voltage ramps (Magistretti & Alonso, 1999; Maurice *et al.* 2001) and in contrast with G_{NaP} , G_{NaPW} is not activated by voltages more depolarized than 0 mV. Thus, a non-window persistent

component (G_{NaP}) was added in the model used for the FDC. This additional component varied between 0.1 and 0.2% of the maximal transient component (3.7 ± 0.3 nS, $n = 5$). A lower maximal conductance was found in ADPNs (0.6 nS) probably because the dissociation had considerably reduced the membrane area and subsequently the number of NaChs.

Depolarizing steps of current were applied to elicit three to four APs. The leftward shift of the activation of the simulated G_{NaP} by 6.5 mV increased the number of spikes ($+319 \pm 100\%$, $n = 5$, Fig. 6C), promoted the production of bursts and decreased the first AP latency ($-36 \pm 2\%$, $n = 5$, Fig. 6D), indicating that excitability was largely enhanced. When the leftward shift of the activation of G_{NaP} was applied in combination with the shift of the inactivation of G_{NaT} by 6 mV, regenerative firing was suppressed (Fig. 6C). The value of 6 mV was chosen because neuronal firing was often difficult to elicit when the shift was greater than 8 mV. Compared to the control, the latency of the first spike was slightly decreased ($-11 \pm 5\%$, $n = 5$, Fig. 6D) but the number of APs was strongly reduced ($-55 \pm 10\%$, $n = 5$, Fig. 6C). We conclude that the mGluR1-dependent regulation of NaChs promotes the spike induction at the threshold but strongly decreases regenerative firing. The net decrease in excitability produced by activation of mGluR subtype 1 is further supported by the fact that pharmacological blockade of mGluR1 enhanced intrinsic excitability. Bath application of the mGluR1 antagonist LY367385 ($100 \mu\text{M}$) increased the number of spikes evoked by a depolarizing current pulse injected in L5 neurons under basal and elevated levels of glutamate release (Fig. 7). Consistent with a glutamate-dependent regulation of intrinsic excitability, LY367385 increased excitability to a greater extent when glutamate release was elevated by bath application of 10 mM KCl ($262 \pm 43\%$, $n = 4$ in KCl *vs.* $129 \pm 2\%$ in control, $n = 3$, Fig. 7). Thus, glutamate depresses neuronal excitability via the mGluR1-dependent regulation of NaCh activity.

Discussion

Regulation of sodium currents by mGluR1

We found here that activation of glutamate receptors induced a $\sim 30\%$ reduction in rapidly inactivating Na^+ current in cortical pyramidal neurons. This ability of the mGluR1/5 agonist DHPG to produce this effect, the absence of effect of the specific mGluR5 agonist and the block of DHPG-induced reduction of I_{NaT} by mGluR1 antagonists LY367385, CPCCOEt and AIDA support the conclusion that this effect is mediated by mGluR1. Immunolabelling has indicated that the α -spliced variant of the mGluR1 subunit is mainly located in the dendrites of cortical pyramidal neurons (Munoz *et al.* 1999) and

on inhibitory interneurons (Baude *et al.* 1993). Thus, it is possible that mGluR1 principally regulates NaChs located in the dendrites (Stuart & Sakmann, 1994).

The reduction of I_{NaT} was fully blocked by the PKC inhibitory peptide 19–36 and by BIS-I, a broad spectrum but specific PKC inhibitor. This result is consistent with several previous studies showing that activation of PKC shifted Na^+ current inactivation to more hyperpolarized potentials (Numann *et al.* 1991; Franceschetti *et al.* 2000; Carr *et al.* 2002). Group I mGluR, which include mGluR1 and mGluR5, are coupled to Gq and to the activation

of phosphoinositide hydrolysis, leading to downstream activation of PKC. It has recently been shown, that the novel PKC ϵ subtype is principally involved in the regulation of NaChs (Chen *et al.* 2005).

Regulation of I_{NaT}

DHPG reduced both the Na^+ current and action potential amplitudes. Activation of mGluR1 produced a -9.5 mV shift in the inactivation of I_{NaT} but no change in its activation. A similar observation was reported upon

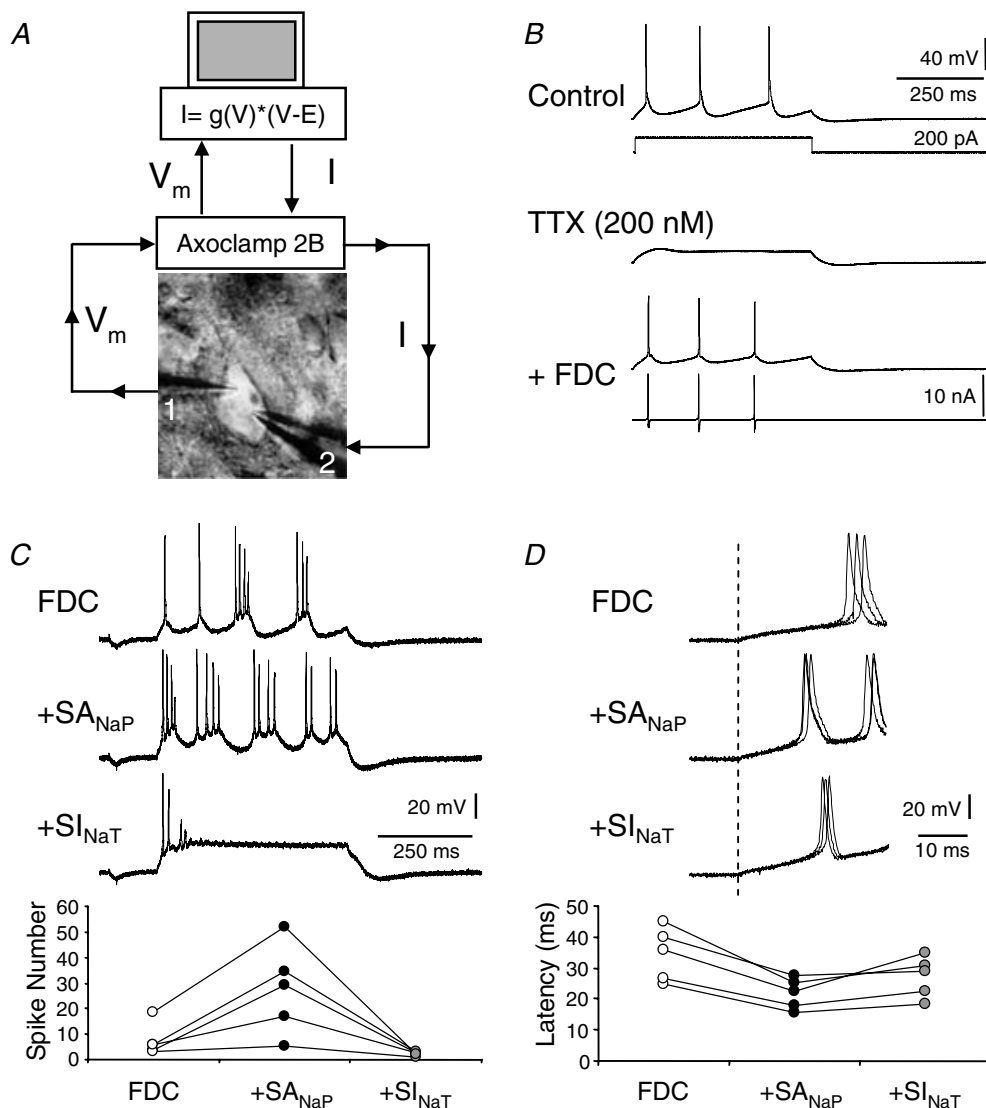


Figure 6. Fast dynamic-clamp (FDC) of Na^+ current in L5 pyramidal neurons

A, experimental set-up for injecting artificial G_{NaT} , G_{NaP} and G_K . A pyramidal neuron was recorded in double whole-cell configuration in a cortical slice. V_m was measured by electrode 1 and the dynamic current, I_{Dyn} , was injected by electrode 2. *B*, validation of FDC in a regular spiking neuron. Top, APs were evoked by a step of depolarizing current. Middle, TTX blocked firing. Bottom, addition of the simulated G_{NaT} , G_{NaP} and G_K with FDC (I_{Dyn}) re-established the discharge. *C* and *D*, FDC in a bursting neuron. Effects of shifting the activation of I_{NaP} (SA_{NaP}) by 6.5 mV and the inactivation of I_{NaT} (SI_{NaT}) by 6 mV on the number of spikes evoked by a depolarizing step (*C*) and the latency of the first AP (*D*). Each data point corresponds to a single neuron.

stimulation of PKC (Franceschetti *et al.* 2000) or 5-HT₂ receptors (Carr *et al.* 2002). Our model shows that this shift is sufficient to produce the reduction in amplitude of I_{NaT} evoked by a voltage step from -70 mV to -20 mV. No change in the activation of I_{NaT} was observed as previously reported upon activation of muscarinic (Cantrell *et al.* 1996) or 5-HT₂ receptors (Carr *et al.* 2002). Functionally, shifting inactivation with the FDC technique reduced repetitive firing. Indeed, although the overall firing was reduced, the latency of the first spike remained virtually unchanged. Similar behaviour has also been observed previously upon stimulation of 5-HT_{2a/c} receptors (Carr *et al.* 2003).

Regulation of I_{NaP}

The shift in I_{NaT} inactivation produced a strong decrease in the amplitude of the theoretical window-current. This behaviour was not exactly observed in the recordings of I_{NaP} . In fact, a decrease in I_{NaP} was observed only for potentials near -40 mV but a clear facilitation was found at -55 mV, indicating that the regulation of I_{NaT} cannot solely account for the changes in I_{NaP} . Thus, transient and persistent components might be mediated by different mechanisms or types of channels. In fact, several biophysical differences are observed between channels generating fast transient and persistent Na⁺ currents. The underlying unitary conductances of single channels are clearly different (15 vs. 20 pS) and the activation threshold of I_{NaP} is 10 mV more hyperpolarized (Magistretti *et al.* 1999). In addition, G-protein $\beta\gamma$ subunits selectively enhance I_{NaP} in a subtype-selective population of NaChs (Mantegazza *et al.* 2005). Although the possibility that I_{NaT} and I_{NaP} are mediated by different channels is still a matter of debate, it is possible that mGluR1 differentially regulates two types of Na⁺ channels. Nevertheless, this regulatory mechanism also required PKC activation since DHPG had no effect on I_{NaP} in the presence of the PKC inhibitor BIS-I.

A similar shift in I_{NaP} activation has been reported following stimulation of PKC (Astman *et al.* 1998; Franceschetti *et al.* 2000) or D₁/D₅ receptors (Gorelova & Yang, 2000). A reduction in I_{NaP} amplitude has been observed in some (Astman *et al.* 1998; Mittmann & Alzheimer, 1998), but not all studies (Franceschetti *et al.* 2000; Gorelova & Yang, 2000; this study). Functionally, this facilitation increased neuronal excitability. In the presence of Ca²⁺ and K⁺ channel blockers, DHPG decreased the latency of the first AP and increased the amplitude of the depolarizing foot preceding the AP. Shifting the activation curve of simulated G_{NaP} by -6.5 mV using the FDC technique produced virtually identical results. Thus, mGluR1-dependent facilitation of I_{NaP} is a powerful means to enhance intrinsic

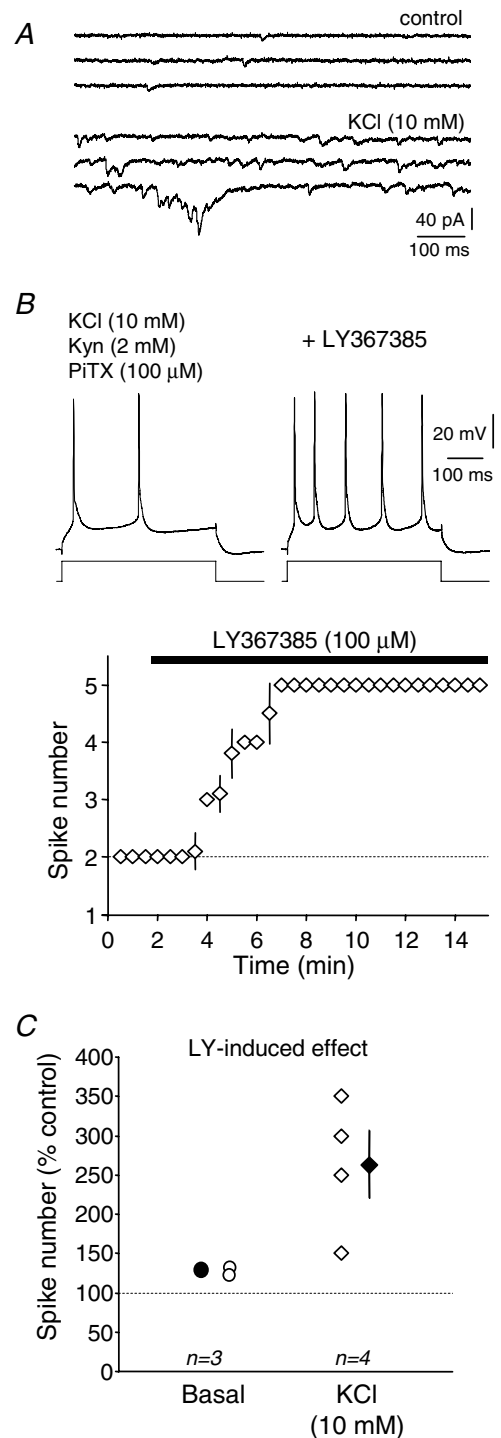


Figure 7. Effects of the mGluR1 antagonist LY367385 on intrinsic excitability of L5 pyramidal neurons

A, spontaneous postsynaptic currents ($V_h = -70$ mV) recorded in control (top traces) and in the presence of 10 mM KCl (bottom traces). B, effect of LY367385 on spiking activity in the presence of 10 mM KCl. Ionotropic receptors were blocked with kynurenat (2 mM) and picrotoxin (100 μM). Bottom, time course of the effect of LY367385. C, normalized changes induced by LY367385 in control conditions (basal) and with an external K⁺ concentration of 10 mM (KCl).

excitability. It will be important to determine whether this glutamate-dependent up-regulation of I_{NaP} might also account for some of the activity-dependent long-lasting changes in intrinsic excitability observed in cerebellar and cortical neurons (Armano *et al.* 2000; Daoudal *et al.* 2002).

Net change in neuronal excitability

Simulation of mGluR1-dependent regulation of NaCh activity with FDC techniques showed a bipolar impact on neuronal excitability. In fact, reduction in repetitive AP firing and facilitation of the first AP latency are the main features of the mGluR1-dependent regulation of NaCh activity. What is their net effect on neuronal excitability? Two different parameters were measured to assess the change in neuronal excitability. In terms of AP number, overall excitability decreased. However, when spike initiation was considered, excitability was enhanced since the first spike latency was reduced. Thus, activation of mGluR1 profoundly affects the temporal dynamics of pyramidal neuron excitability.

Whether GPCR/PKC-dependent regulation of NaCh activity increases or decreases neuronal excitability is a matter of debate. Excitability might be decreased because of I_{NaT} depression (Cantrell & Catterall, 2001; Carr *et al.* 2002) or enhanced as a result of facilitation of I_{NaP} (Astman *et al.* 1998; Franceschetti *et al.* 2000). Furthermore, the depression of excitability is questionable since M_1 , D_1/D_2 , $5HT_2$ and mGluR1 not only regulate NaChs but also modulate a wide variety of K^+ and Ca^{2+} channels that are clearly involved in determining neuronal excitability (Malenka & Nicoll, 1986; Charpak *et al.* 1990; Anwyl, 1999; Mannaioni *et al.* 2001). Thus, the consequences of metabotropic receptor stimulation on excitability are difficult to dissect with classical tools. We were able to address this issue by the use of FDC. In fact, the specific changes in NaCh activity induced by mGluR1 stimulation could be reconstituted in real neurons. Endogenous NaChs were selectively blocked with TTX and the simulated Na^+ conductance was injected in the recorded neuron. The FDC technique has, however, limitations: the injected conductance is restricted to the site of current injection (Prinz *et al.* 2004) and FDC of Na^+ current probably does not restore active back-propagation in the dendrites. Thus, activation of Na^+ - and Ca^{2+} -dependent K^+ channels is reduced. G_K was added to reduce bursting caused by the reduction of Na^+ -dependent K^+ currents (Bhattachardjee & Kaczmarek, 2005) due to TTX. Shifting activation of simulated G_{NaP} enhanced excitability but when the shift in the inactivation of G_{NaT} was added, excitability was strongly decreased. The fact that the mGluR1 antagonist LY367385 increased neuronal excitability in L5 pyramidal neurons further argues for a net decrease in excitability mediated by mGluR1-dependent regulation of NaCh.

Functional implication

Given the importance of Na^+ channels and glutamate in brain function, it is expected that regulation of NaCh activity will have important functional consequences postsynaptically. Group I mGluRs are involved in the patterning of epileptiform activity in cortical neurons (Merlin & Wong, 1997; Merlin, 2002). In particular, mGluR1 activation underlies the acute enhancement of epileptiform bursts whereas mGluR5 is involved in the sustained increase in neuronal excitability (Merlin, 2002; Stoop *et al.* 2003; Sourdet *et al.* 2003). Our data are consistent with the implication of mGluR1 in the maintenance of recurrent epileptiform activity via an action on I_{NaP} . In fact, the shift of the activation of I_{NaP} may increase EPSP amplification and facilitate the generation of APs in response to weak EPSPs (Stuart & Sakmann, 1995). At the scale of a neuronal ensemble, this process might promote epileptiform activity. Indeed, augmentation of I_{NaP} may produce spontaneous seizures (Kearney *et al.* 2001).

However, the mGluR1-dependent regulation of I_{NaT} produced a strong reduction of regenerative firing. This dominant effect might participate in the homeostatic regulation of neuronal excitability in the cortex. In fact, postsynaptic mGluR1/5 down-regulate a wide variety of K^+ currents, thereby increasing repetitive firing of APs (Charpak *et al.* 1990; Guérineau *et al.* 1994; Lüthi *et al.* 1996; Anwyl, 1999; Mannaioni *et al.* 2001). This hyper-excitability could be largely reduced by the mGluR1-dependent regulation of I_{NaT} we described here. Thus, mGluR1-dependent regulation of Na^+ current may represent a novel mechanism of homeostatic regulation acting during intense glutamatergic synaptic activity (Desai, 2003). Consistent with this, the mGluR1 antagonist LY367385 enhanced intrinsic excitability in an activity-dependent manner. The magnitude of the effect was significantly larger when glutamatergic activity was stimulated by high external K^+ . However, basal levels of glutamate also regulate excitability of cortical neurons (Bandrowski *et al.* 2003).

The mGluR1-dependent regulation of NaCh may also have important functional consequences at the presynaptic side. Activation of mGluR1 inhibits excitatory synaptic transmission via a presynaptic mechanism that remains unclear (Mannaioni *et al.* 2001). Na^+ channels have been identified in excitatory presynaptic terminals (Engel & Jonas, 2005). Thus, one possible mechanism of the mGluR1-dependent inhibition of evoked glutamate release might reside in the fact that presynaptic transient Na^+ currents are inhibited by the activation of mGluR1. Additional experiments will be necessary to further determine whether mGluR1-mediated reduction of the I_{NaT} may promote propagation failures (Debanne, 2004) or reduce the amplification of the presynaptic action potential (Engel & Jonas, 2005).

References

- Anwyl R (1999). Metabotropic glutamate receptors: electrophysiological properties and role in plasticity. *Brain Res Rev* **29**, 83–120.
- Armano S, Rossi P, Taglietti V & D'Angelo E (2000). Long-term potentiation of intrinsic excitability at the mossy fiber-granule cell synapse of rat cerebellum. *J Neurosci* **20**, 5208–5216.
- Astman N, Gutnick MJ & Fleidervish IA (1998). Activation of protein kinase C increases neuronal excitability by regulating persistent Na⁺ current in mouse neocortical slices. *J Neurophysiol* **80**, 1547–1551.
- Bandrowski AE, Huguenard JR & Prince DA (2003). Baseline glutamate levels affect group I and II mGluRs in layer V pyramidal neurons of rat sensorimotor cortex. *J Neurophysiol* **89**, 1308–1316.
- Baude A, Nusser Z, Roberts JDB, Mulvihill E, McIlhinney RAJ & Somogyi P (1993). The metabotropic glutamate receptor (mGluR1a) is concentrated at perisynaptic membrane of neuronal subpopulation as detected by immunogold reaction. *Neuron* **11**, 771–787.
- Bhattachardjee A & Kaczmarek LK (2005). For K⁺ channels, Na⁺ is the new Ca²⁺. *Trends Neurosci* **28**, 422–428.
- Cantrell AR & Catterall WA (2001). Neuromodulation of Na⁺ channels: an unexpected form of cellular plasticity. *Nat Rev Neurosci* **2**, 397–407.
- Cantrell AR, Ma JY, Scheuer T & Catterall WA (1996). Muscarinic modulation of sodium current by activation of protein kinase C in rat hippocampal neurons. *Neuron* **16**, 1019–1026.
- Cantrell AR, Scheuer T & Catterall WA (1997). Dopaminergic modulation of sodium current in hippocampal neurons via cAMP-dependent phosphorylation of specific sites in the sodium channel α subunit. *J Neurosci* **17**, 7330–7338.
- Cantrell AR, Tibbs VC, Westenbroek RE, Scheuer T & Catterall WA (1999). Dopaminergic modulation of voltage-gated Na⁺ current in rat hippocampal neurons requires anchoring of cAMP-dependent protein kinase. *J Neurosci* **19**, RC21.
- Carlier E, Dargent B, De Waard M & Couraud F (2000). Na⁺ channel regulation by calmodulin kinase II in rat cerebellar granule cells. *Biochem Biophys Res Comm* **274**, 394–399.
- Carr DB, Cooper DC, Ulrich SL, Spruston N & Surmeier DJ (2002). Serotonin receptor activation inhibits sodium current and dendritic excitability in prefrontal cortex via a protein kinase C-dependent modulation. *J Neurosci* **22**, 6846–6855.
- Carr DB, Day M, Cantrell AR, Held J, Scheuer T, Catterall WA & Surmeier DJ (2003). Transmitter modulation of slow, activity-dependent alterations in sodium channel availability endows neurons with a novel form of cellular plasticity. *Neuron* **39**, 793–806.
- Chapack S, Gähwiler BH, Do KQ & Knopfel T (1990). Potassium conductances in hippocampal neurons blocked by excitatory amino-acid transmitters. *Nature* **347**, 765–767.
- Chen Y, Cantrell AR, Messing RO, Scheuer T & Catterall WA (2005). Specific modulation of Na⁺ channels in hippocampal neurons by protein kinase C ϵ . *J Neurosci* **25**, 507–513.
- Chuang SC, Bianchi R & Wong RKS (2000). group I mGluR activation turns on a voltage-gated current in hippocampal pyramidal cells. *J Neurophysiol* **83**, 2844–2853.
- Conn PJ & Pin JP (1997). Pharmacology and functions of metabotropic glutamate receptors. *Annu Rev Pharmacol Toxicol* **37**, 205–237.
- Daoudal G, Hanada Y & Debanne D (2003). Bi-directional plasticity of excitatory postsynaptic potential (EPSP)-spike coupling in CA1 hippocampal pyramidal neurons. *Proc Natl Acad Sci U S A* **99**, 14512–14517.
- Debanne D (2004). Information processing in the axon. *Nat Rev Neurosci* **5**, 304–316.
- Desai NS (2003). Homeostatic plasticity in the CNS: synaptic and intrinsic forms. *J Physiol (Paris)* **97**, 391–402.
- Engel D & Jonas P (2005). Presynaptic action potential amplification by voltage-gated Na⁺ channels in hippocampal mossy fiber boutons. *Neuron* **45**, 405–417.
- Fleidervish IA, Friedman A & Gutnick MJ (1996). Slow inactivation of Na⁺ current and slow cumulative spike adaptation in mouse and guinea-pig neocortical neurons in slices. *J Physiol* **493**, 83–97.
- Franceschetti S, Taverna S, Sancini G, Panzica F, Lombardi R & Avanzini G (2000). Protein kinase C-dependent modulation of Na⁺ currents increases the excitability of rat neocortical pyramidal neurons. *J Physiol* **528**, 291–304.
- Gorelova NA & Yang CR (2000). Dopamine D1/D5 receptor activation modulates a persistent sodium current in rat prefrontal cortical neurons in vitro. *J Neurophysiol* **84**, 75–87.
- Guérineau NC, Gähwiler BH & Gerber U (1994). Reduction of resting K⁺ current by metabotropic glutamate and muscarine receptors in rat CA3 cells: mediation by G-proteins. *J Physiol* **474**, 27–33.
- Hilborn MD, Vaillancourt RR & Rance SG (1998). Growth factor receptor tyrosine kinases regulate neuronal sodium channels through the Src signaling pathway. *J Neurosci* **18**, 590–600.
- Huguenard JR, Hamill OP & Prince DA (1988). Developmental changes in Na⁺ conductances in rat neocortical neurons: appearance of a slowly inactivating component. *J Neurophysiol* **59**, 778–795.
- Kearney JA, Plummer NW, Smith MR, Kapur J, Cummins TR, Waxman SG, Goldin AL & Meisler MH (2001). A gain-of-function mutation in the sodium channel gene *Scn2a* results in seizures and behavioral abnormalities. *Neuroscience* **102**, 307–317.
- Kullmann PHM, Wheeler DW, Beacom J & Horn JP (2004). Implementation of a fast 16-bit dynamic clamp using LabView-RT. *J Neurophysiol* **91**, 542–554.
- Li M, West JW, Lai Y, Scheuer T & Catterall WA (1992). Functional modulation of brain sodium channels by cAMP-dependent phosphorylation. *Neuron* **8**, 1151–1159.
- Lien CC & Jonas P (2003). Kv3 potassium conductance is necessary and kinetically optimized for high-frequency action potential generation in hippocampal interneurons. *J Neurosci* **23**, 2058–2068.
- Lüthi A, Gähwiler BH & Gerber U (1996). A slowly inactivating potassium current in CA3 pyramidal cells of rat hippocampus in vitro. *J Neurosci* **16**, 586–594.

- Magistretti P & Alonso A (1999). Biophysical properties and slow voltage-dependent inactivation of a sustained sodium current in entorhinal cortex layer-II principal neurons: a whole-cell and single-channel study. *J General Physiol* **114**, 491–509.
- Magistretti J, Ragsdale DS & Alonso A (1999). High conductance sustained single-channel activity responsible for the low-threshold persistent Na⁺ current in entorhinal cortex neurons. *J Neurosci* **19**, 7334–7341.
- Malenka RC & Nicoll RA (1986). Dopamine decreases the calcium-activated afterhyperpolarization in hippocampal CA1 pyramidal cells. *Brain Res* **379**, 210–215.
- Mannaioni G, Marino MJ, Valenti O, Traynelis SF & Conn J (2001). Metabotropic glutamate receptors 1 and 5 differentially regulate CA1 pyramidal cell function. *J Neurosci* **21**, 5925–5934.
- Mantegazza M, Hu FH, Powell AJ, Clare JJ, Catterall WA & Scheuer T (2005). Molecular determinants for modulation of persistent sodium current by G-protein $\beta\gamma$ subunits. *J Neurosci* **25**, 3341–3349.
- Maurice N, Tkatch T, Meisler M, Sprunger LK & Surmeier DJ (2001). D1/D5 dopamine receptor activation differentially modulates rapidly inactivating and persistent sodium currents in prefrontal cortex pyramidal neurons. *J Neurosci* **21**, 2268–2277.
- Merlin LR (2002). Differential roles for mGluR1 and mGluR5 in the persistent prolongation of epileptiform bursts. *J Neurophysiol* **87**, 621–625.
- Merlin LR & Wong RKS (1997). Role of group I metabotropic glutamate receptors in the patterning of epileptiform activities in vitro. *J Neurophysiol* **78**, 539–544.
- Mittmann T & Alzheimer C (1998). Muscarinic inhibition of persistent Na⁺ current in rat neocortical pyramidal neurons. *J Neurophysiol* **79**, 1579–1582.
- Munoz A, Lu X & Jones EG (1999). Development of metabotropic glutamate receptors from trigeminal nuclei to barrel cortex in postnatal mouse. *J Comp Neurol* **409**, 549–566.
- Numann R, Catterall WA & Scheuer T (1991). Functional modulation of brain sodium channels by protein kinase C phosphorylation. *Science* **254**, 115–118.
- Prinz AA, Abbott LF & Marder E (2004). The dynamic clamp comes of age. *Trends Neurosci* **27**, 218–224.
- Ratcliff CF, Qu Y, McCormick KA, Tibbs VC, Dixon JE, Scheuer T & Catterall WA (2000). A sodium channel signaling complex: modulation by associated receptor protein tyrosine phosphatase β . *Nat Neurosci* **3**, 437–444.
- Schwindt PC & Crill WE (1995). Amplification of synaptic current by persistent sodium conductance in apical dendrite of neocortical neurons. *J Neurophysiol* **74**, 2220–2224.
- Sigel E & Baur R (1988). Activation of protein kinase C differentially modulates neuronal Na⁺, Ca²⁺ and γ -aminobutyrate type A channels. *Proc Natl Acad Sci U S A* **85**, 6192–6196.
- Sourdet V, Russier M, Daoudal G, Ankri N & Debanne D (2003). Long-term enhancement of neuronal excitability and temporal fidelity mediated by metabotropic glutamate receptor subtype 5. *J Neurosci* **23**, 10238–10248.
- Stoop R, Conquet F, Zuber B, Voronin LL & Pralong E (2003). Activation of metabotropic glutamate 5 and NMDA receptors underlies the induction of persistent bursting and associated long-lasting changes in CA3 recurrent connections. *J Neurosci* **23**, 5634–5644.
- Stuart GJ & Sakmann B (1994). Active propagation of somatic action potentials into neocortical pyramidal neurons. *Nature* **367**, 69–72.
- Stuart GJ & Sakmann B (1995). Amplification of EPSPs by axosomatic sodium channels in neocortical pyramidal neurons. *Neuron* **15**, 1065–1077.
- Wittmack EK, Rush AM, Hudson A, Waxman SG & Dib-Hajj SD (2005). Voltage-gated sodium channel Nav1.6 is modulated by p38 mitogen-activated protein kinase. *J Neurosci* **25**, 6621–6630.

Acknowledgements

We thank O. Caillard, R. Cudmore and M. Seagar for constructive criticisms on the manuscript and L. Savtchenko for advice on the model. We thank M. Seagar for his constant support. This work was supported by INSERM (AVENIR and Postdoctoral grant to P.D.), CNRS, Fondation pour la Recherche Médicale and the Ministry of Research (Doctoral grants to V.S. and S.B. and ACI Jeunes Chercheurs).

Supplemental material

The online version of this paper can be accessed at:
 DOI: 10.1113/jphysiol.2006.118026
<http://jp.physoc.org/cgi/content/full/jphysiol.2006.118026/DC1>
 and contains supplemental material consisting of three figures:

Supplemental Figure 1. Hodgkin-Huxley-type model of the sodium current

Supplemental Figure 2. Dose-response curve of the DHPG-induced inhibition of the transient current

Supplemental Figure 3. Effects of mGluR5 CHPG (100 or 200 μ M) on intrinsic excitability of L5 pyramidal neurons